JCTC Journal of Chemical Theory and Computation

What Is the Limit of Atom Encapsulation for Icosahedral Carboranes?

Vanesa Manero and Josep M. Oliva*

Instituto de Química-Física Rocasolano (CSIC), ES-28006 Madrid, Spain

Luis Serrano-Andrés

Instituto de Ciencia Molecular, Universidad de Valencia, ES-46100 Valencia, Spain

Douglas J. Klein

Texas A&M University at Galveston, Galveston, Texas 77553-1675

Received February 19, 2007

Abstract: The stability of endohedral carboranes X@{1,*n*-$C_2B_{10}H_{12}$} (X = Li^+, Be^{2+}; *n* = 2, 7, 12) and X@{$CB_{11}H_{12}^-$} (X = Li^+, Be^{2+}) is studied using electronic structure calculations with the B3LYP/6-311+G(d,p) model. Our calculations suggest that all endohedral compounds are local energy minima; for the exohedral complexes X···cage, the global energy minimum always corresponds to the X atom above a triangular face of the icosahedron. In the latter the X atom is furthest apart from the carbon atoms of the cage. As opposite to exohedral {Be^{2+}···cage} complexes, no global energy minima were found for exohedral complexes {Li^+···cage} whereby a carbon atom is present in the triangular face of the icosahedron below the Li^+ cation.

1. Introduction

To our knowledge, no reports on the syntheses of endohedral carboranes have appeared in the bibliography to date.[1] The potential applications of these complexes within such research fields as nanotechnology or biology are still to be investigated: While fullerene-derived endohedral complexes have been thoroughly studied since the first detection of C_{60},[2] with prediction of insertion and ejection mechanisms for the endohedral atoms,[3,4] this is not the case with carborane-derived endohedral compounds. Atom-filled carbon nanotubes and fullerene boxes have been proposed as superconductors, drug-delivery agents, and 3D atom carriers under different control forms.[5−7] In a recent work, a nanoencapsulation of two o-carborane molecules has been carried out through BC−H···π hydrogen bonds in a ball-and-socket structure.[8] What should we then expect for endohedral complexes derived from carboranes? In a recent work, an ejection mechanism of the endohedral atom viable for the Li^+@$CB_{11}H_{12}^-$ system was proposed on theoretical grounds.[9] On the other hand, related guest systems derived from the monoanion $[CB_{11}H_{12}]^-$, such as the stable weakly nucleophilic anion $[CB_{11}Me_{12}]^-$, have been synthesized with an inner negative charge prone to accept cationic species.[10] Predictions on novel stuffed polyhedral boranes $(X@B_{12}H_{12})^n$ have been previously published,[1,11,12] but we are not aware of similar reports considering carborane clusters as guest systems as the ones we propose in the current report. In this work we present a computational study on the stabilities and geometries of exohedral (X···cage) and endohedral (X@cage) icosahedral carboranes derived from ortho-carborane, meta-carborane, para-carborane, the monoanion $CB_{11}H_{12}^-$, and the cations X = {Li^+, Be^{2+}}.

2. Computational Method

All the calculations in this work were performed at the B3LYP/6-31G(d) and B3LYP/6-311+G(d, p) level of theory with the suite of programs Gaussian03.[13] Energy minima were characterized by computing second derivatives and harmonic vibrational frequencies used to obtain zero point vibrational energy (ZPE) corrections, at the same level of theory. The global energy minima for the exo complexes X···cage were found after posititioning the X atom above

10.1021/ct700042z CCC: $37.00
Published on Web 06/16/2007

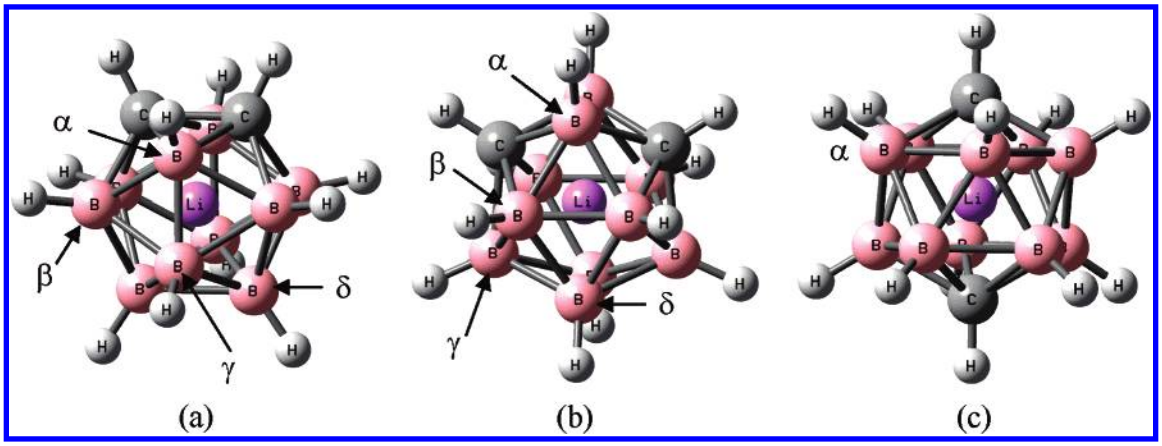

Figure 1. Optimized geometries of (a) Li^+@o-carborane (**1a**), (b) Li^+@m-carborane (**1b**), and (c) Li^+@p-carborane (**1c**). All calculations are at the B3LYP/6-311+G(d, p) level of theory. All geometries correspond to energy minima.

Table 1. Selected Distances (Å), Energies (au), Zero-Point Energy (ZPE) Corrections (kcal/mol), and Strain Energies E^c (kcal/mol) in Compounds **1a**−**c** and **3a**−**c** Computed at the B3LYP/6-311+G(d, p) Level of Theory

compound	C···C	Li···C	Li···B_α	Li···B_β	Li···B_γ	Li···B_δ	*E*	ZPE	E^c
1a	1.712	1.712	1.836	1.789	1.750	1.727	−339.218643	108.7	183.1
1b		1.673	1.831[a]	1.787[a]	1.756[a]	1.741[a]	−339.240692	109.7	181.1
1c		1.644[a]	1.783[a]				−339.241376	109.9	177.2
compound	C···C	Be···C	Be···B_α	Be···B_β	Be···B_γ	Be···B_δ	*E*	ZPE	E^c
3a	1.701	1.778	1.901	1.804	1.729	1.687	−345.989878	105.6	135.8
3b		1.692	1.898[a]	1.802[a]	1.751[a]	1.713[a]	−346.009676	105.8	128.7
3c		1.637[a]	1.800[a]				−346.007415	105.6	118.8

[a] Average of Li/Be···B/C distances.

all nonequivalent triangular faces of the respective icosahedron and checking energies and frequencies of all optimizations; the global energy minimum of the X···cage structure corresponds to the system with lowest energy and all positive frequencies. Only results from the B3LYP/6-311+G(d, p) calculations are included in this work since the conclusions reached are identical for both basis sets.

3. Results and Discusion

3.1. Endohedral Systems X@carborane. *3.1.1. Li^+@{o-carborane}, Li^+@{m-carborane}, and Li^+@{p-carborane}.* The optimized geometries of the endohedral carboranes derived from Li^+ and o-carborane (**1a**), m-carborane (**1b**), and p-carborane (**1c**) are shown in parts a−c, respectively, of Figure 1. The optimized structures depicted in Figure 1 all correspond to energy minima.

Table 1 gathers selected geometrical parameters and energies of the endo compounds displayed in Figure 1 (the optimized geometries of all systems in this work are included in the Supporting Information).

A comprehensive computational study of the dependence of C···C distances in o-carboranes as a function of the substituents on the C's in the cage was recently published.[14] The computed C−C bond distance in o-carborane is R_{CC} = 1.627 Å-B3LYP/6-311+G(d, p) calculations—the experimental value is R_{CC} =1.629 Å.[15] As shown in Table 1, when a Li^+ atom is introduced in the o-carborane cage, the C···C distance increases by ∼0.09 Å. In **1a** the two carbon atoms and the Li atom form an equilateral triangle. In **1b** and **1c** the Li···C distance decreases as compared to **1a** by ∼0.04 Å and ∼0.07 Å, respectively. The most noticeable change in the remaining parameters included in Table 1 are the Li···B_α distances, the latter decreasing for **1c** as compared to **1a** in ∼0.05 Å. An enhanced stability is thus evidenced from o-carborane to p-carborane when a Li^+ atom is introduced in the cage, as in the case of simple o-carborane, m-carborane, and p-carborane, where the energy order is *E*(o-carborane) < *E*(m-carborane) < *E*(p-carborane).

3.1.2. Be^{2+}@{o-carborane}, Be^{2+}@{m-carborane}, and Be^{2+}@{p-carborane}. The optimized geometries of the endohedral carboranes derived from Be^{+2+} and o-carborane (**3a**), m-carborane (**3b**), and p-carborane (**3c**) are shown in parts a−c, respectively, of Figure 2. All optimized structures depicted in Figure 2 correspond to energy minima.

As shown in Figure 2 and Table 1, the endohedral complexes derived from Be^{2+} and o-carborane, m-carborane, and p-carborane are stable structures from the energetical point of view (all correspond to local energy minima). The C···C distance in **3a** is even smaller than in the Li analogue (**1a**), by ∼0.01 Å. However, for ortho and meta derivatives the cages show larger X···B parameters for α and *β* boron atoms with X = Be^{2+}. This behavior is opposite for *γ* and *δ* boron atoms as shown in Table 1. Note that the energetic order in **3a**−**c** is now *E*(**3b**) < *E*(**3c**) < *E*(**3a**), as opposed to the neutral and endohedral complexes derived from Li^+, where the sequence is *E*(**3c**) < *E*(**3b**) < *E*(**3a**).

3.2. Exohedral X···Cage Systems. *3.2.1. Global Minima in Li^+···{Carborane} Complexes.* In section 2.1 we showed that the endodedral compounds X@carborane—with X = {Li^+, Be^{2+}} and carborane = {o-carborane, m-carborane,

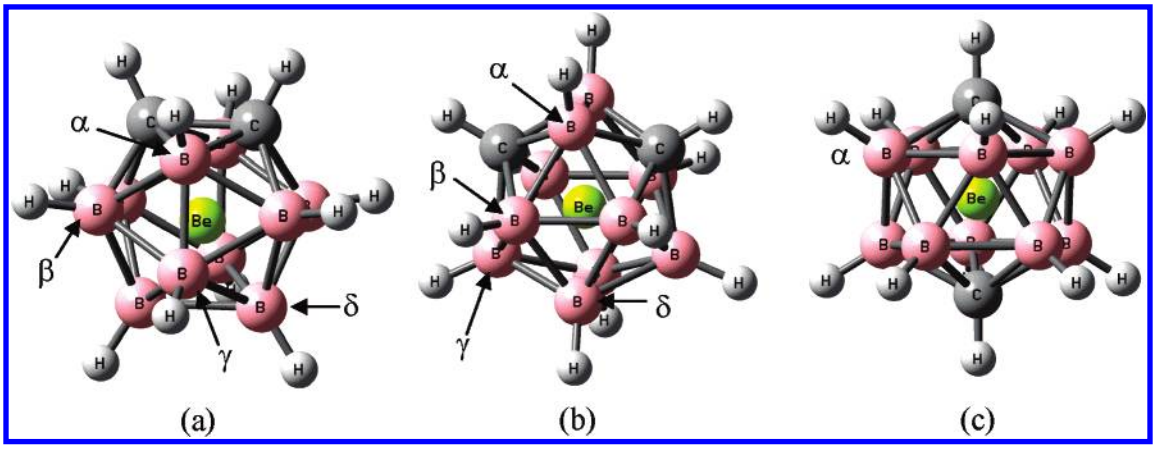

Figure 2. Optimized geometries of (a) Be^{2+}@o-carborane (**3a**), (b) Be^{2+}@m-carborane (**3b**), and (c) Be^{2+}@p-carborane (**3c**). All calculations are at the B3LYP/6-31G* level of theory. All geometries correspond to energy minima.

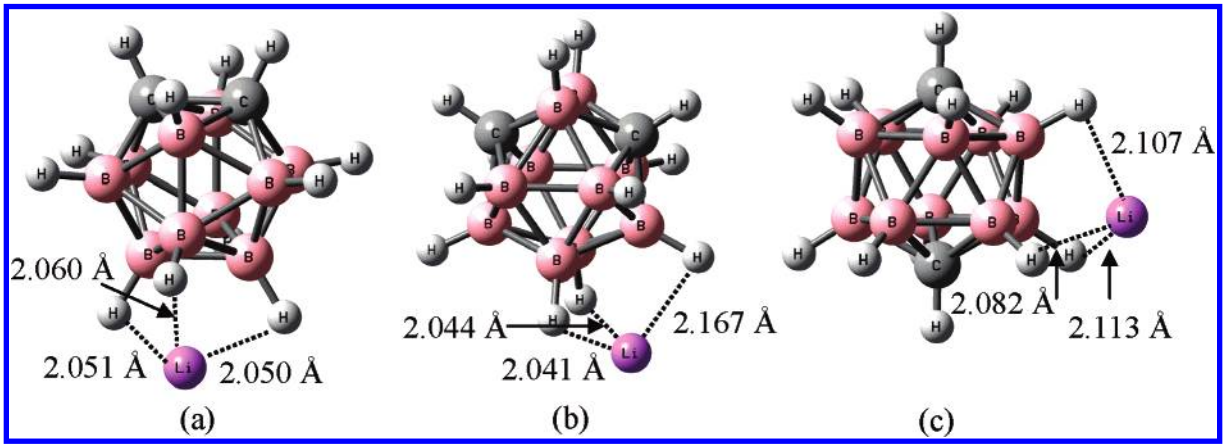

Figure 3. Optimized geometries of the exohedral complex $Li^{+}\cdots$cage (a) $Li^{+}\cdots${o-carborane} (**2a**), (b) $Li^{+}\cdots${m-carborane} (**2b**), and (c) $Li^{+}\cdots${p-carborane} (**2c**). All calculations are at the B3LYP/6-311+G(d, p) level of theory. All geometries correspond to energy minima. Also displayed are the closest Li···H distances.

p-carborane}—corresponded to local energy minima. Similar endohedral compounds derived from fullerenes have been observed and synthesized[16,17] since the first detection of C_{60} more than 20 years ago.[2] A comprehensive search of energies on the surface of o-carborane, m-carborane, and p-carborane and the Li^{+} cation showed that the global energy minima of the complex $Li^{+}\cdots$cage corresponds to the structures displayed in Figure 3.

Other local minima were found above the triangular faces of the boron cage, but they were always higher in energy as compared to the structures displayed in Figure 3: the global minimum is always in the triangular face of the icosahedron furthest apart from any of the carbon atoms in the cage, regardless of the carborane isomer. No triangular faces in complexes **2a** and **2c** containing at least one carbon atom correspond to energy minima. However, this is not the case for the meta complex **2b**. Table 2 gathers the energetics and zero-point energy corrections for the complexes displayed in Figure 3.

The lowest energy complex corresponds to the meta isomer: E(**2b**) < E(**2c**) < E(**2a**). A B3LYP/6-311+G(d, p) calculation on Li−H results in a distance R(Li−H) = 1.592 Å; in the radical cation $(Li-H)^{\bullet+}$, the computed distance is R = 2.188 Å. Therefore the situation displayed in Figure 3, with regards to Li···H distances, is closer to the radical cation

Table 2. Energies (au) and Zero-Point Energy (ZPE) Corrections (kcal/mol) for Exo Complexes **2a**−**c** and **4a**−**c** Computed at the B3LYP/6-311+G(d, p) Level of Theory

compound	*E*	ZPE
2a	−339.510368	111.8
2b	−339.529334	111.9
2c	−339.523684	111.8
4a	−346.206304	111.6
4b	−346.214700	111.5
4c	−346.196739	111.1

$(Li-H)^{\bullet+}$ rather than to the neutral Li−H system; we should also take into account the multiple coordination of the Li^{+} cation around the carborane cage, as usual for this cation.[18]

3.2.2. Global Minima in $Be^{2+}\cdots${Carborane} Complexes. Turning now to the Be^{2+} cation, we also performed a comprehensive search for energy minima around the carborane cage surface and this cation. Figure 4 shows the global minima obtained from the interaction of Be^{2+} and o-carborane, m-carborane, and p-carborane leading to complexes **4a**−**c**, respectively.

A B3LYP/6-311G+(d, p) geometry optimization on BeH_2 gives R(Be−H) = 1.327 Å. For the radical cation $(BeH_2)^{\bullet+}$, the same calculation gives R(Be−H) = 1.413 Å. As for the dication, the optimization results in a C_{2v} $Be^{2+}\cdots(H_2)$

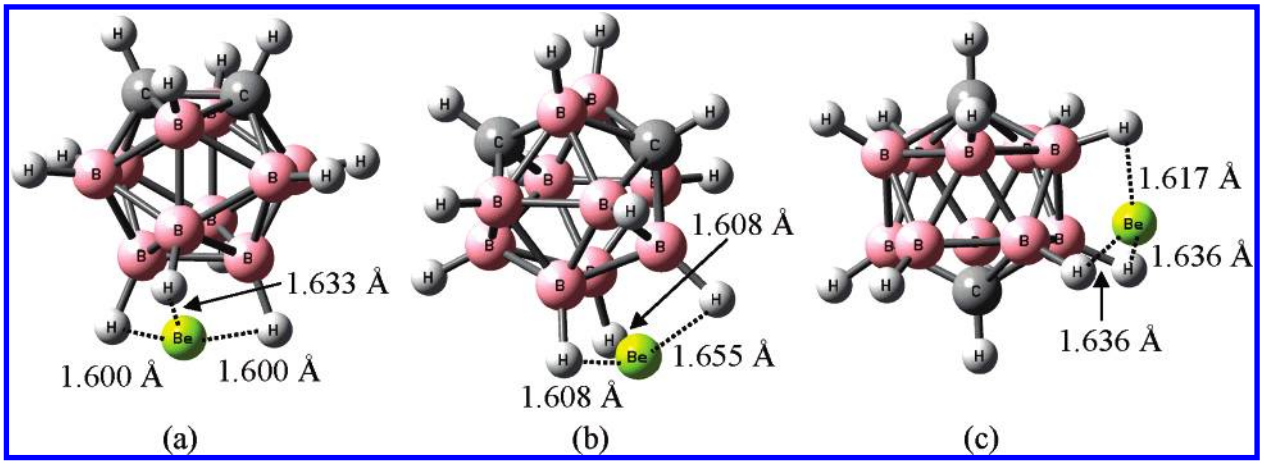

Figure 4. Optimized geometries of the exohedral complex $Be^{2+}\cdots$cage (a) $Be^{2+}\cdots$\{o-carborane\} (**4a**), (b) $Be^{2+}\cdots$\{m-carborane\} (**4b**), and (c) $Be^{2+}\cdots$\{p-carborane\} (**4c**). All calculations are at the B3LYP/6-311+G(d, p) level of theory. All geometries correspond to energy minima. Also displayed are the closest Be···H distances.

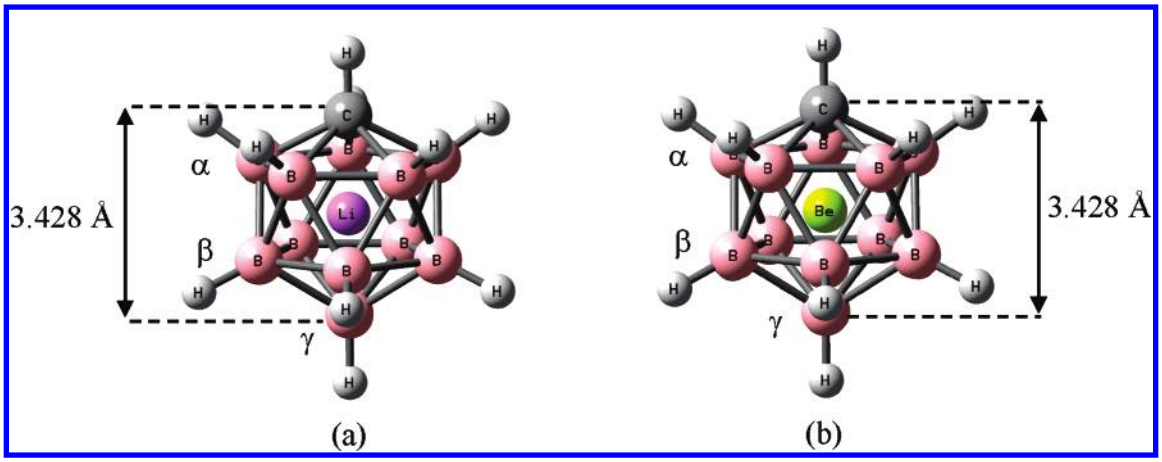

Figure 5. Optimized geometries of the endohedral complexes (a) $Li^+@\{CB_{11}H_{12}^-\}$ (**5**) and (b) $Be^{2+}@\{CB_{11}H_{12}^-\}$ (**7**). All calculations are at the B3LYP/6-311+G(d, p) level of theory. All geometries correspond to energy minima.

complex with R(H−H) = 0.821 Å and R(Be−H) = 1.629 Å. The computed frequency for this complex corresponding to the H···H stretching is 3516 cm^{-1}; for isolated H_2, this computed frequency is 4416 cm^{-1} (R(H−H) = 0.744 Å), and for the radical cation $(H_2)^{\bullet+}$, 2051 cm^{-1} (R(H−H) = 1.108 Å). We can thus deduce that the bonding situation derived from the complexes $Be^{2+}\cdots$cage **4a**−**c** corresponds—at least from the Be···H distances—more closely to a $(Be^{2+})\cdot\cdot\cdot$(H) attractive interaction rather than a Be−H bond. Note that the Be···H distances in the exo complexes are ∼0.5 Å smaller than in the exo Li complexes (see Figure 3). The energies and ZPE corrections for exo Be complexes are gathered in Table 2: The energetic order is E(**4b**) < E(**4a**) < E(**4c**), which is different from the exo Li complexes. Finally, we should point out that we found other local energy minima (higher in energy than those displayed in Figure 4) with Be^{2+} above triangular faces of the icosahedron where one or two carbon atoms are present in the face: As mentioned above, this is not the case for the exo Li-derived complexes.

3.3. Endohedral Complexes X@\{$CB_{11}H_{12}^-$\}, X = \{Li^+, Be^{2+}\}. We turn now to the endohedral systems derived from the monoanion $\{CB_{11}H_{12}^-\}$ and the cations Li^+ and Be^{2+}. Figure 5 shows the optimized structures for $Li^+@\{CB_{11}H_{12}^-\}$ (**5**) and $Be^{2+}@\{CB_{11}H_{12}^-\}$ (**7**). The labels for the corresponding exo complexes (see section 2.4) $Li^+\cdots\{CB_{11}H_{12}^-\}$ and $Be^{2+}\cdots\{CB_{11}H_{12}^-\}$ are **6** and **8**, respectively.

As shown in Figure 5, the encapsulation of Li^+ or Be^{2+} inside $CB_{11}H_{12}^-$ hardly changes the apical distances between C and B_γ. In **7**, the Be atom is pushed down far from C, ∼0.02 Å as compared to **5**, and closer to B_γ. From the values of Table 3, we can deduce that the X···C and X···B_α distances in **5** are smaller than in **7**; however, for X···B_β and X···B_γ the situation is inverted, with longer distances for **5** as compared to **7**. In other words it is apparent that Be^{2+} is pushed toward the lower part of the carborane cage as compared to the Li^+ endohedral complex.

3.4. Exohedral Complexes X···\{$CB_{11}H_{12}^-$\}, X = \{Li^+, Be^{2+}\}. Figure 6 depicts the optimized structures of the global energy minima derived from Li^+ and Be^{2+} and the monoanion $CB_{11}H_{12}^-$: $Li^+\cdots\{CB_{11}H_{12}^-\}$ (**6**) and $Be^{2+}\cdots\{CB_{11}H_{12}^-\}$ (**8**).

Comparison of Figure 3 and Figure 6a shows that the Li atom is closer to the cage by ∼0.10−0.15 Å as compared to the exo complex derived from neutral carboranes, which can be attributed to the negative charge of the cage monoanion, since the Mulliken charges on Li (in units of |e|) for **2a**−**c**

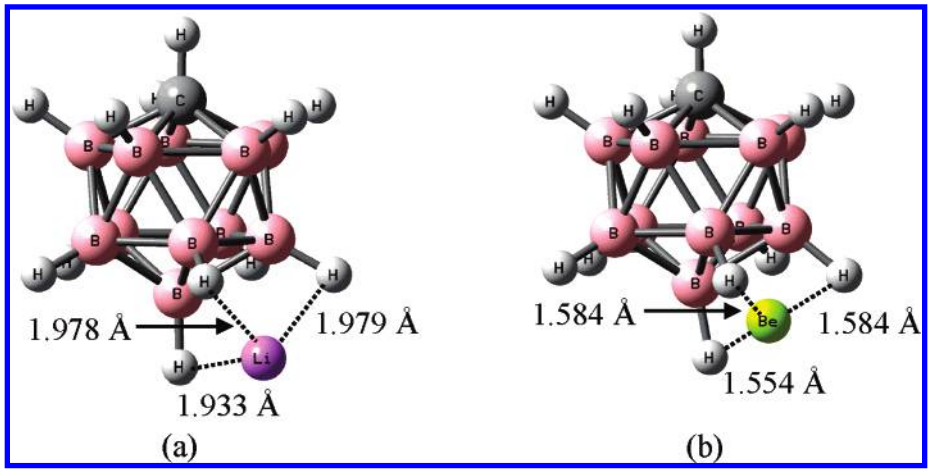

Figure 6. Optimized geometries of the exohedral complexes corresponding to global energy minima (a) $Li^+\cdots\{CB_{11}H_{12}^-\}$ (**6**) and (b) $Be^{2+}\cdots\{CB_{11}H_{12}^-\}$ (**8**). All calculations are at the B3LYP/6-311+G(d, p) level of theory.

Table 3. Selected Distances, Energies (au), Zero-Point Energy (ZPE) Corrections (kcal/mol), and Strain Energies E^c (kcal/mol) for Endohedral Complexes and Exohedral Complexes $Li^+@\{CB_{11}H_{12}^-\}$ = **5**, $Li^+\cdots\{CB_{11}H_{12}^-\}$ = **6**, $Be^{2+}@\{CB_{11}H_{12}^-\}$ = **7**, and $Be^{2+}\cdots\{CB_{11}H_{12}^-\}$ = **8**[a]

compound	X···C	X···B_α	X···B_β	X···B_γ	*E*	ZPE	E^c
5	1.692	1.802[b]	1.762[b]	1.736	−326.301887	108.7	149.9
7	1.722	1.830[b]	1.750[b]	1.706	−333.256216	106.0	96.7
6					−326.540828	109.8	
8					−333.410348	110.1	

[a] All computations with the B3LYP/6-311+G(d, p) model. [b] Average of Li/Be···B/C distances.

and **6** are as follows: q_{Li}(**2a**) = 0.68, q_{Li}(**2b**) = 0.68, q_{Li}(**2c**) = 0.68, and q_{Li}(**6**) = 0.56.

As for the exo Be complex (**8**), comparison of Figures 4 and 6 shows a decrease of the Be···H distance by ∼0.05 Å as compared to the exo neutral complexes **4a**−**c**. Again, this can be fairly attributed to the compensation of charges between the anion and the cation: q_{Be}(**4a**) = 0.36, q_{Be}(**4b**) = 0.38, q_{Be}(**4c**) = 0.36, and q_{Be}(**8**) = 0.21.

Again, the charge on Be has been reduced almost to half from the exo neutral carborane complexes **4** to the exo complex **8** with the carborane monoanion $CB_{11}H_{12}^-$.

3.5. Strain Energies. In this section we analyze the strain energies E^c, which are defined as the difference between the exohedral and endohedral structures. The strain energies indicate the amount by which the exohedral species are energetically more favorable than the endohedral complexes. As indicated in Table 1 (last column), the strain energies for the Li complexes with the neutral carboranes are 50−60 kcal/mol larger than the Be counterparts, hence indicating an "easier" path (at least thermodynamically) toward the encapsulated complex for the latter. Turning to the complexes derived from Li^+ and Be^{2+} and the monoanion $CB_{11}H_{12}^-$—Table 3—the strain energies are smaller than in the previous complexes **1** and **3**. For Li^+ and Be^{2+} complexes, the differences in strain energies range from 30 to 35 kcal/mol for the Li^+ complexes and 20−40 kcal/mol for the Be^{2+} complexes when the latter interact with the neutral (ortho, meta, and para) and monoanionic carboranes.

4. Conclusions

The optimized structures for the endohedral and exohedral complexes derived from the interaction of Li^+ and Be^{2+} cations with icosahedral neutral and monoanionic carboranes are reported using the B3LYP/6-311+G(d, p) model. All endohedral structures reported correspond to local energy minima with a range of strain energies. With regards to exohedral structures, as opposed to Be^{2+} complexes, a comprehensive energy minimum search shows that for Li^+ no energy minima are found whereby a carbon atom is present in the triangular face of the icosahedron. We hope that the results presented in this work encourage new forthcoming routes toward the experimental syntheses of the endohedral compounds $\{X@C_nB_{12-n}H_{12}\}^{n-2}$ (n = 1,2), (X = Li^+, Be^{2+}).

Acknowledgment. This work was financed under project MAT2006-13646-C03-02 from the Spanish Ministry of Science and Education. J.M.O. is grateful to Professor Neil L. Allan (University of Bristol, U.K.) for helpful discussions.

Supporting Information Available: Optimized geometries of all systems. This material is available free of charge via the Internet at http://pubs.acs.org.

References

(1) Jemmis, E. D.; Balakrishnarajan, M. M. *J. Am. Chem. Soc.* **2000**, *122*, 7392−7393.

(2) Kroto, H. W.; Heath, J. R.; O'Brien, S. C.; Curl, R. F.; Smalley, R. E. *Nature* **1985**, *318*, 162−163.

(3) Murry, R. L.; Scuseria, G. E. *Science* **1994**, *263*, 791−793.

(4) Yumura, T.; Sato, Y.; Suenaga, K.; Urita, K.; Iijima, S. *Nano Lett.* **2006**, *6*, 1389−1395.

(5) Tenne, R. *Nature* **2004**, *431*, 640−641.

(6) Regan, B. C.; Aloni, S.; Ritchie, R. O.; Dahmen, U.; Zettl, A. *Nature* **2004**, *428*, 924−927.

(7) Lee, J.; Kim, H.; Kahng, S.-J.; Kim, G.; Son, Y.-W.; Ihm, J.; Kato, H.; Wang, Z. W.; Okazaki, T.; Shinohara, H.; Kuk, Y. *Nature* **2002**, *415*, 1005−1008.

(8) Raston, C. L.; Cave, G. W. V. *Chem. Eur. J.* **2004**, *10*, 279−282.

(9) Serrano-Andrés, L.; Oliva, J. M. *Chem. Phys. Lett.* **2006**, *432*, 235−239.

(10) King, B. T.; Janoušek, Z.; Grüner, B.; Trammell, M.; Noll, B. C.; Michl, J. *J. Am. Chem. Soc.* **1996**, *118*, 3313−3314.

(11) Charkin, O. P.; Klimenko, N. M.; Moran, D.; Mebel, A. M.; Charkin, D. O.; Schleyer, P. v. R. *J. Phys. Chem. A* **2002**, *106*, 11594−11602.

(12) Charkin, O. P.; Klimenko, N. M.; Moran, D.; Mebel, A. M.; Charkin, D. O.; Schleyer, P. v. R. *Inorg. Chem.* **2001**, *40*, 6913−6922.

(13) Frisch, M. J.; Trucks, G. W.; Schlegel, H. B.; Scuseria, G. E.; Robb, M. A.; Cheeseman, J. R.; Montgomery, J. A., Jr.; Vreven, T.; Kudin, K. N.; Burant, J. C.; Millam, J. M.; Iyengar, S. S.; Tomasi, J.; Barone, V.; Mennucci, B.; Cossi, M.; Scalmani, G.; Rega, N.; Petersson, G. A.; Nakatsuji, H.; Hada, M.; Ehara, M.; Toyota, K.; Fukuda, R.; Hasegawa, J.; Ishida, M.; Nakajima, T.; Honda, Y.; Kitao, O.; Nakai, H.; Klene, M.; Li, X.; Knox, J. E.; Hratchian, H. P.; Cross, J. B.; Bakken, V.; Adamo, C.; Jaramillo, J.; Gomperts, R.; Stratmann, R. E.; Yazyev, O.; Austin, A. J.; Cammi, R.; Pomelli, C.; Ochterski, J. W.; Ayala, P. Y.; Morokuma, K.; Voth, G. A.; Salvador, P.; Dannenberg, J. J.; Zakrzewski, V. G.; Dapprich, S.; Daniels, A. D.; Strain, M. C.; Farkas, O.; Malick, D. K.; Rabuck, A. D.; Raghavachari, K.; Foresman, J. B.; Ortiz, J. V.; Cui, Q.; Baboul, A. G.; Clifford, S.; Cioslowski, J.; Stefanov, B. B.; Liu, G.; Liashenko, A.; Piskorz, P.; Komaromi, I.; Martin, R. L.; Fox, D. J.; Keith, T.; Al-Laham, M. A.; Peng, C. Y.; Nanayakkara, A.; Challacombe, M.; Gill, P. M. W.; Johnson, B.; Chen, W.; Wong, M. W.; Gonzalez, C.; Pople, J. A. *Gaussian 03, Revision C.02*; Gaussian, Inc.: Wallingford, CT, 2004.

(14) Oliva, J. M.; Allan, N. L.; Schleyer, P. v. R.; Viñas, C.; Teixidor, F. *J. Am. Chem. Soc.* **2005**, *127*, 13538−13547.

(15) Davidson, M. G.; Hibbert, T. G.; Howard, J. A. K.; Mackinnon, A.; Wade, K. *Chem. Commun.* **1996**, *19*, 2285−2286.

(16) Bethune, D. S.; Johnson, R. D.; Salem, J. R.; de Vries, M. S.; Yannoni, C. S. *Nature* **1993**, *366*, 123−128.

(17) Wang, C.-R.; Dennis, J. S.; Inakuma, M.; Shinohara, H. In *Fullerenes: Recent Advances in the Chemistry and Physics of Fullerenes and Related Materials*; Kadish, K. M., Ruoff, R. S., Eds.; Electrochemical Society: Pennington, 1998; pp 1023−1030.

(18) *Lithium Chemistry: A Theoretical and Experimental Overview*; Sapse, A.-M., Schleyer, P. v. R., Eds.; Wiley: 1995.

CT700042Z